Structures 8 (2016) 25–34

Contents lists available at ScienceDirect

Structures

journal homepage: www.elsevier.com/locate/structures

Effect of Inconsistent Diaphragms on Exterior Girder Rotation During Overhang Deck Construction

Md Ashiquzzaman [a], Li Hui [a], Ahmed Ibrahim Ph.D., P.E. [b,*], Will Lindquist Ph.D., P.E. [c], Mark Thomson P.E., S.E. [d], Riyadh Hindi Ph.D., P.Eng., F.SEI [e]

[a] Parks College of Engineering, Aviation and Technology, Saint Louis University, St. Louis, MO 63103, USA
[b] Department of Civil Engineering, University of Idaho, Moscow, ID 83844, USA
[c] William Jewell College, Liberty, MO 64068, USA
[d] Bureau of Bridges & Structures Design & Construction Review Unit Chief, Illinois Department of Transportation, Springfield, IL, USA
[e] Parks College of Aviation, Engineering and Technology, Saint Louis University, St. Louis, MO 63103, USA

ARTICLE INFO

Article history:
Received 12 May 2016
Received in revised form 13 July 2016
Accepted 3 August 2016
Available online 5 August 2016

Keywords:
Deck overhang
Exterior girder rotation
Screed machine
Non-skewed bridge
Steel girder
Asymmetric diaphragm

ABSTRACT

The construction of bridge deck overhangs results in unbalanced eccentric loads acting on exterior girders which can cause rotation and increased stresses not accounted for during design. Permanent diaphragms and temporary bracing in bridge exterior girder lines or panels are used to resist these loads and subsequent transverse rotation of the exterior girders. The addition of extra diaphragms in the exterior panels is one potential alternative to temporary bracing which is not always effective. In this paper, a unique steel plate girder bridge in the state of Illinois with extra diaphragms in one exterior bay was instrumented with tilt sensors and strain gages to monitor transverse rotations and strains due to unbalanced loads occurring during construction. Two types of rotations were recorded; maximum and residual rotations. The extra diaphragms were included in the design of this bridge on only one side of the bridge to carry utility lines. The full bridge was modeled using the commercial finite element analysis software ABAQUS and the model was validated using field data. As expected, diaphragm spacing was found to have a high impact on exterior girder rotations that occur during bridge deck construction. The maximum obtained finite element rotation was 0.47° which occurred at mid span and on the bridge deck side that does not have extra diaphragms. Field residual rotations were found higher (approximate 50% on average) than rotation determined from the finite element analysis. These extra stable rotations were seen in the exterior girders and was a result of permanent deformation occurring when the finishing screed passed by the section under consideration.

1. Introduction

Bridge engineers generally use the fewest number of steel girders possible across the roadway width to reduce construction costs. In nearly every case, bridge deck extends past the exterior girders to increase the effective width of the deck. The extended width or deck overhang is shown in Fig. 1. During construction, loads from the plastic concrete and construction equipment on the overhang deck can cause excessive exterior girder rotation leading to a loss of deck thickness as well as instabilities during construction, to name a few.

The overhang deck formwork is supported by steel brackets resting against the exterior girders at a spacing of 120 cm (4 ft) to 180 cm (6 ft) over the full length of the bridge (shown in Fig. 2). The main function of these brackets is to transfer the overhang construction loads to the exterior girders. If the girders are not properly braced, these loads can lead to changes in deck thickness as well as local and global instabilities [1]. Steel plate girders with slender webs subjected to axial loads are inherently susceptible to instability or buckling [2,3] making local instabilities a major concern for plate girder bridges subject to additional eccentric loads [4,5,6,7]. On the other hand, global instability is a significant issue for concrete girders where their rotational stiffness leads to rigid body rotation [8,9]. There have been several studies to evaluate commercially available overhang brackets and hangers to limit rotation [10,11,12], although girder rotation continues to be a concern.

Rotations in exterior girders primarily depend on the geometric and structural properties of the plate girder [13,14,15]. Determining the transverse rotation of exterior girders and characterizing the effect of the rotation on the bridge is a crucial issue for bridge designers and construction engineers. In construction, girder rotations are affected by the bridge geometry, torsional stiffness of the girders, the lateral support system, and the connection details [16,17]. In particular, rotation (as

* Corresponding author.
E-mail address: aibrahim@uidaho.edu (A. Ibrahim).

http://dx.doi.org/10.1016/j.istruc.2016.08.002
2352-0124/

Fig. 1. Overhang deck in a typical steel girder bridge.

shown in Fig. 3) primarily depends on the overhang deck width, diaphragm spacing, total construction loads acting on the deck overhang, and the effectiveness of the lateral bracing system used to prevent rotation during construction. In general, construction loads include the weight of fresh concrete, screed rails, overhang formwork, and construction live loads. It is possible to reduce the load effect by placing the screed rails directly over the exterior girders rather than placing them on the overhang formwork. However, most contractors prefer to place the rails on the overhang formwork to simplify concrete placement, consolidation and finishing [18] as shown in Fig. 4.

Increasing the width of the overhang deck results in a larger eccentricity which increases the torsional moment applied to the exterior girders. In the United States, the width of the overhang deck varies, but most states place some limit on their width. Generally, the maximum allowable overhang width is based on some combination of girder spacing, girder depth, and deck thickness. Exterior girder rotations are generally prevented through the use of temporary bracing systems that transfer the eccentric loads to the girders without inducing significant rotations. Several types of systems are available to contractors. One system used in Illinois includes No. 13 (No. 4) steel reinforcing bars placed parallel to the transverse reinforcement and connected to the top exterior girder flanges as shown in Fig. 5. These tie bars are usually placed at 120 cm (4 ft) to 180 cm (6 ft) intervals along the span of the bridge. Permanent diaphragms providing lateral stability and load transfer between girders also play a significant role in controlling exterior girder rotation. Specifically, the spacing between diaphragms (including intermediate diaphragms located between bridge bents) is a primary factor that dictates their effectiveness in resisting transverse deformation under unbalanced eccentric loads [19]. They are usually spaced 7.62 m (25 ft) apart.

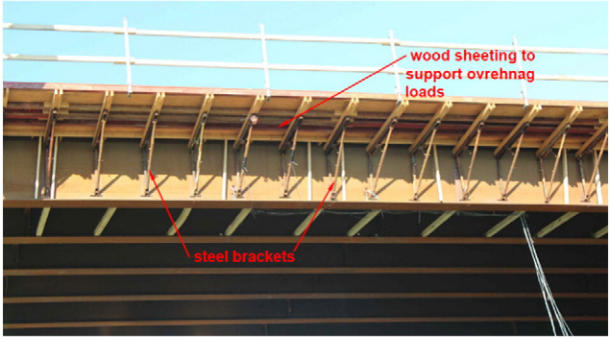

Fig. 2. Overhang deck formed by wood sheathing supported with cantilever steel brackets.

Diaphragms are traditionally placed uniformly across the width of the bridge connecting each girder. This provides continuity that is necessary to resist lateral forces (e.g., wind, earthquake, etc.) and to distribute gravity loads. However, there are some circumstances that warrant permanent diaphragms in the exterior girder panels only (rather than across the entire deck) as shown in Figs. 6 and 7 where the diaphragms are used to provide structural support for utility conduits. This inconsistent or non-continuous diaphragm pattern in exterior panels also represents a potential solution to limit exterior girder rotations. The main objective of this paper is to present the results of field-monitored rotation data for a bridge with inconsistent diaphragms in the exterior panels. Finite element analysis is performed and compared to the field data providing bridge and construction engineers with a better understanding of exterior girder rotations due to eccentric loads in the presence of additional diaphragms in exterior superstructure panels.

2. Bridge description

The bridge selected for this research is a 122 cm (48 in.) deep non-skewed plate girder bridge in the state of Illinois, USA. The continuous two-span bridge is 70 m (230 ft) in length and has integral abutments. Additional geometric details for the bridge are given in Table 1. A plan view of the bridge, girder elevations, and the diaphragm detailing are shown in Figs. 8, 9 and 10, respectively.

3. Data analysis

During construction of the deck, both inward and outward rotation of the exterior girders was measured as shown in Fig. 3. Outward girder rotations (transverse direction) are taken as positive rotation and inward rotations (transverse direction) are negative. Simple exponential smoothing (SES) was used to filter the field data (time vs. rotation) where the SES equation is given in Eq. (1).

$$\hat{x}_{j+1} = ax_j + (1-a)\hat{x}_j \tag{1}$$

where $\hat{x}_j$is the known series values for time period j, x_j is the forecast value of the variable X for time period j, $\hat{x}_{j+1}$ is the forecast value for time period and a is the smoothing constant [20].

The Statistical Package for the Social Sciences (SPSS) software is used to calculate the peak "maximum rotation" and "residual/permanent/stable rotation" of the girder as shown in Fig. 11. The "maximum rotation" of any particular section occurs when all of the construction loads [screed and finishing machine, fresh concrete (placed up to that section from one end of the deck), and other live loads] are placed at that section. The "residual/permanent/stable rotation" (shown in Fig. 11) for any section is determined after finishing placement of the deck and when all of the live loads are removed leaving only the weight of the fresh concrete. A "limit rotation" is assigned (shown in Table 1) based upon the maximum deflection ($\Delta = 4.76$ mm) at the tip of overhang deck as suggested by IDOT bridge design manual.

4. Field Data Monitoring

4.1. Instrumentation plan

Three transverse sections (S1, S2, and S3) were identified for instrumentation as shown in Fig. 12. At each of these sections, tilt sensors were placed on an exterior girder web and bottom flange and on the web of the first interior girder. Two strain gages were placed on the top transverse tie as shown in Fig. 13.

4.2. Dual-axis tilt sensor

Dual-axis (CXTLA02) tilt sensors capable of measuring rotation in the transverse and longitudinal directions were used to monitor girder

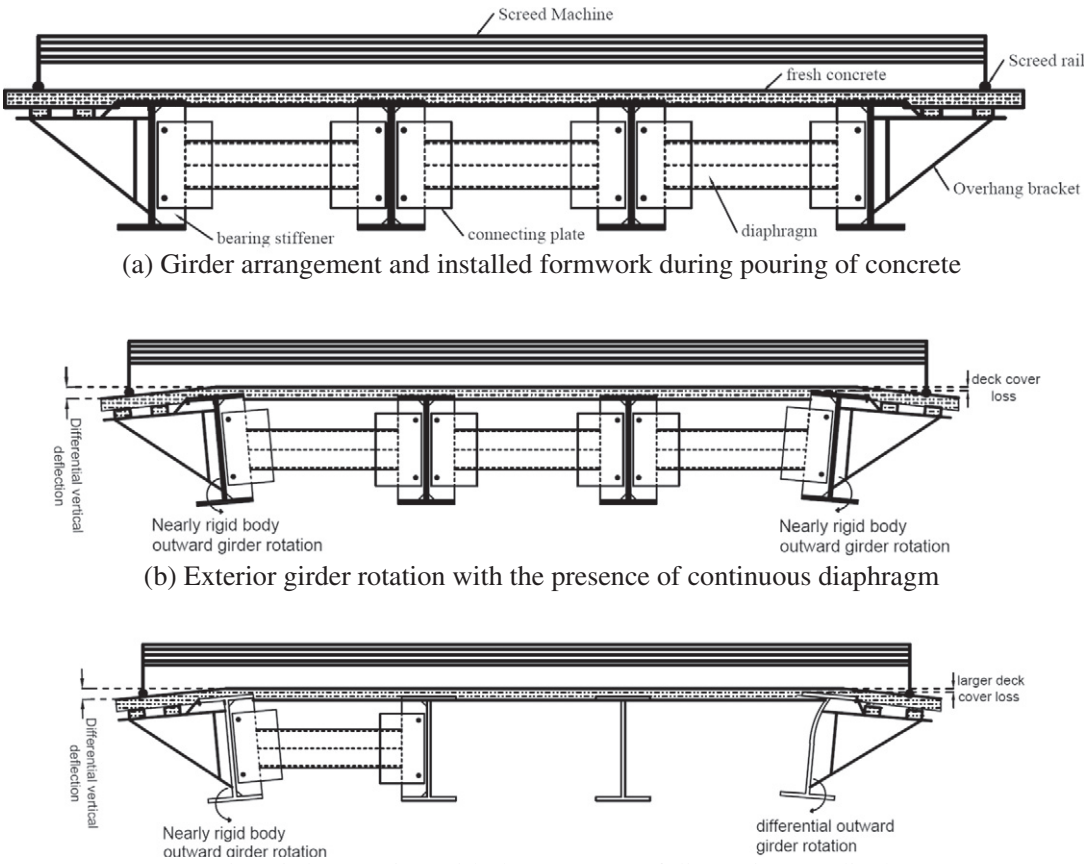

Fig. 3. Exterior girder rotation due to unbalanced eccentric load on overhang deck with inconsistent diaphragm; (a) girder arrangement and installed formwork during pouring of concrete, (b) exterior girder rotation with the presence of continuous diaphragm, (c) exterior girder rotation with the presence of discontinuous diaphragm.

rotations at several locations as shown in Fig. 14. The sensitivity of the tilt sensors was tested prior to field installation. The maximum range of the tilt sensors is 20° as recommended by the manufacturer. Extra care was given to attach the tilt sensors during assembly in both the longitudinal and transverse directions. An open aluminum box was made to hold the tilt sensor as shown in Fig. 14. Quick setting glue was used to attach the aluminum box to the girder. Directions (transverse direction: along the width of the deck and longitudinal direction: along the length of the span) of the tilt sensors were carefully maintained during its installation to avoid misinterpretation in the data analysis.

4.3. Strain gages

Foil strain gages (CEA-06-125UN-350/P2) were installed on the transverse bracing bars (shown in Fig. 15) to measure the strain induced in the bracing bars during and after concrete placement.

4.4. Field data

4.4.1. Girder rotation

It is expected to have the rotations of the two exterior girders vary because of the presence of additional end diaphragms on only one

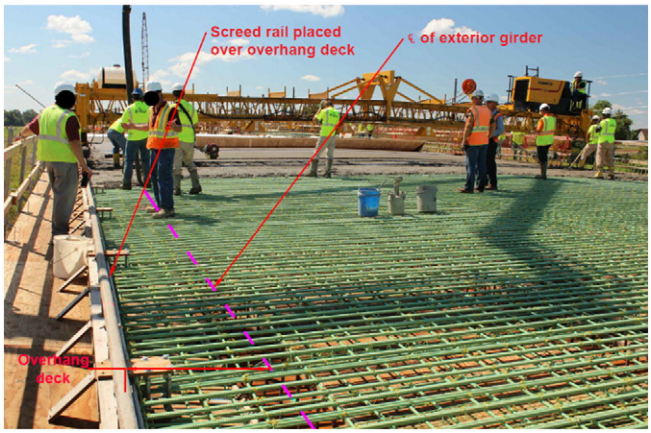

Fig. 4. Screed rail placed on the overhang formwork.

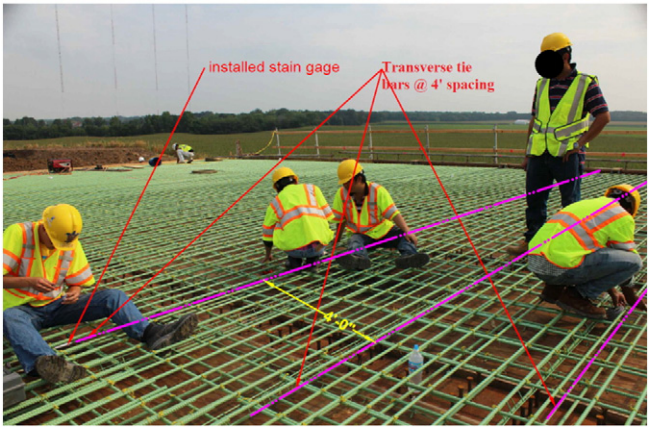

Fig. 5. Transverse tie bars placed at 1.22 m (4 ft) spacing.

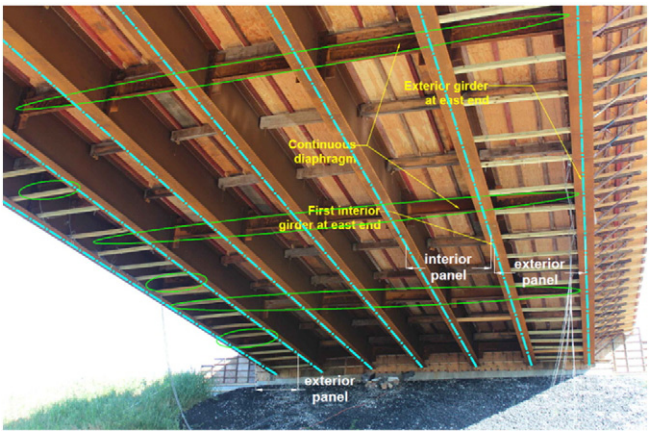

Fig. 6. Exterior girders on the east end of the bridge.

Table 1
Geometric specifications of the bridge.

Bridge type	Non-skewed plate girder bridge
Girder type	1.22 m (48 in.) Plate girder
Number of span	2
Number of girders	7
Girder spacing	2.23 m (7 ft–4 in.)
Diaphragms at both exterior panels	Asymmetric
Overhang width	0.90 m (2 ft–11.5 in.)
Bracing system	Transverse tie bars connecting exterior girder to exterior girder
Screed type	Screed machine
Screed location	On overhang deck
Limit rotation (θ)	30°

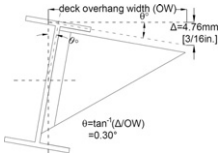

side of the deck (as shown in Fig. 8). The maximum exterior girder rotations for section S1 (shown in Fig. 16) with an intermediate diaphragm at the west end of the bridge are 0.20° and 0.22° at the bottom flange and web locations, respectively. Stable rotations measured upon completion of the deck placement at the bottom flange and the web are 0.15° and 0.14°, respectively. From the maximum and stable rotation of the exterior girder at the west end of the bridge, it can be deduced that the girder tilted as a rigid body. The maximum and stable rotations of the first interior girder on the west side of the deck are 0.13° and 0.11°, respectively, which are also very similar to each other. Unfortunately, the tilt sensors installed on the east exterior girder of the bridge malfunctioned during the deck placement and rotations were not recorded.

Exterior girder rotations in section S2 with a continuous diaphragm (shown in Fig. 12) across the entire width of the bridge are shown in Fig. 17. At the west end, the maximum rotations of the exterior girder at the bottom flange is found 0.2° and the web is 0.25°, and the stable rotations were almost have same trend for both the bottom flange and the web (approx. 0.15°). At the east end, however, the maximum rotation of the exterior girder at the bottom flange and the web are 0.22° and 0.25°, respectively, and the stable rotations at the bottom flange and the web are 0.14° and 0.19°, respectively. Comparing rotations of the east and west exterior girders, it can be seen that the rotations at the east end experienced slightly higher differential rotations between the bottom flange and the web of the girder. This behavior might be attributed to unbalanced tie rods and differences in the temporary timber blocks installed between the two sides along the cross section of the bridge.

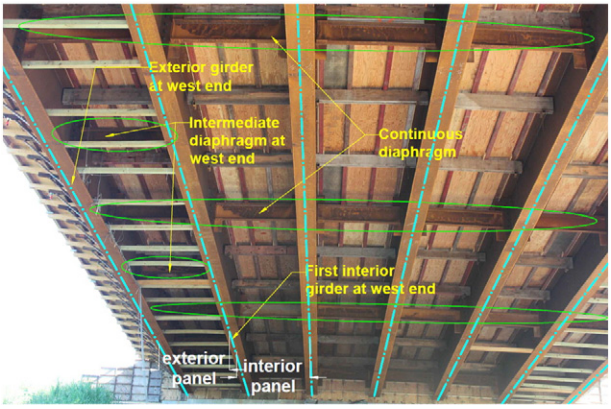

Fig. 7. Exterior girders on the west end of the bridge.

Section S3 (shown in Fig. 18) only has an intermediate diaphragm at the west end where no diaphragms are installed (as shown in Fig. 12). The west exterior girder again shows rigid body rotation where the maximum rotations at the bottom flange and web are 0.16° and 0.17°, respectively. The field exterior girder at the east end (without extra intermediate diaphragm) showed comparatively higher maximum (nearly 0.19°) and stable 0.14° rotations in the bottom flange location of the girder, it can be seen that the difference in both maximum and stable rotations are very small compared to sections S1 and S2.

4.4.2. Stress/strain in tie bars

Transverse bracing bars play an additional supporting role in reducing the exterior girder rotations during deck placement. The effectiveness of the bracing system depends on the size of the tie bars and their connections with the girders. For this bridge, No. 13 (No. 4) steel bars are used as transverse tie bars connected to both exterior girder flanges. A steel hanger [21] was clamped with the exterior girders (shown in Fig. 19) with threaded nuts to tighten the transverse tie bars with hangers. Proper tightening of these nuts is important to ensure full utilization of the tie bars. Some tie bars were observed in the field to sag either due to the self-weight of tie bar or due to interference with other deck reinforcement. Improper tightening and interference with other elements likely reduces the effectiveness of the transverse bracing system. To find out the effectiveness of the transverse tie bars, strain gages were installed as shown in Fig. 15 and extra care was taken to limit impact on the stain gages during concrete placement.

In Fig. 20, the maximum measured strain (stress) in the tie bar at section S1 during construction was 142 μ-strain 28.3 MPa (4.12 ksi) with a stable strain (stress) of 72 μ-strain 14.4 MPa (2.09 ksi).

5. Finite element analysis

5.1. Bridge modeling

A full scale bridge was modeled using ABAQUS 6.14 as shown in Fig. 21(a) and a cross section showing one of the exterior girder and the first interior girder elements is shown in Fig. 21(b). In ABAQUS, the steel girders [121.92 cm (48 in.) plate girder] and the steel diaphragms (C15 × 40) were modeled using shell elements (S4R). Tie constraints were used to connect the diaphragms with the girders. Steel brackets and hangers were modeled as beam (B31) and truss (T3D2) elements. Tie constraints were used to connect the girder's web surface to brackets, brackets to hangers, and hangers to the girder's flange. Transverse tie bars were assembled as truss (T3D2) elements where one end of the tie bars were connected to the top flange of the girder using tie

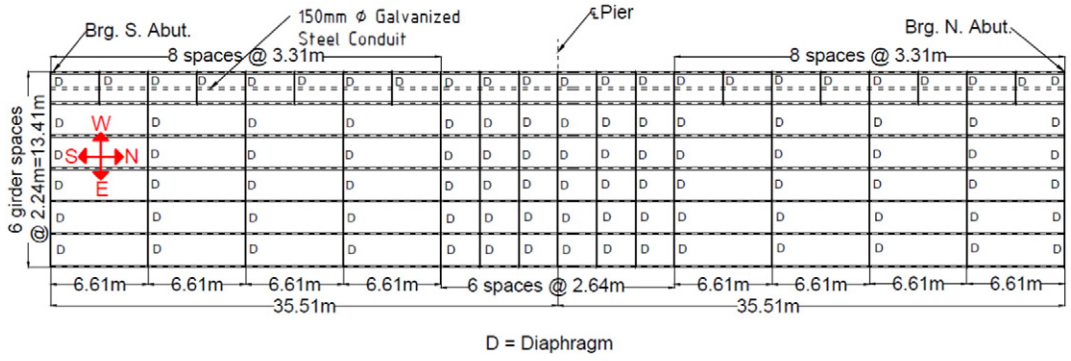

Fig. 8. Plan of the bridge.

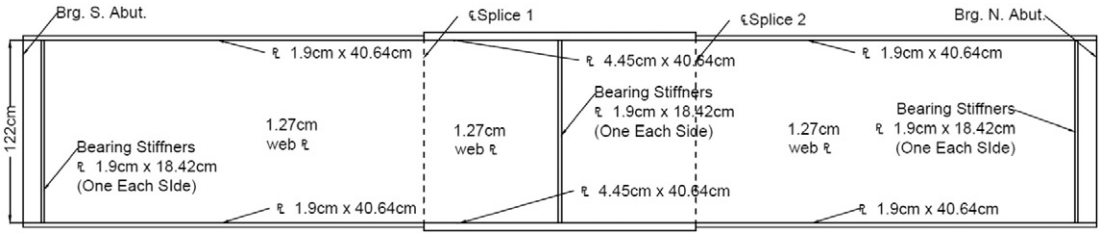

Fig. 9. Elevation of the bridge.

constraints. During construction, the transverse tie bars were frequently observed to sag due to interference with the deck reinforcement or loose connections which can reduce the effectiveness of the tie bar. A link (translator link) element was used to connect transvers tie bars and girders with a "gap" assigned to the link element to allow the girder to move freely up to 2.54 mm (0.10 in.). The gap in the link element simulates the effect of sagging and untightened transverse ties during placement. In this case, the link connectors start to be effective (holding force) when the transverse displacement of the exterior girder exceeds the "gap". The 100 mm × 100 mm (4 in. × 4 in.) timber blocks were represented by truss elements working only under compression. Link (translator link) elements were used to connect the timber blocks and girders where a "gap" was assigned to the link element. The gap modeled between the timber block and the girder was used to simulate improper shimming between timber blocks and girders (shown in Fig. 22) frequently observed during actual bridge construction.

The concrete deck load [exterior girders: 0.0132 N/mm^2 (1.914 psi) and interior girders: 0.0264 N/mm^2 (3.828 psi)] was applied directly to the top flange of the girders. The concrete loads from the overhanging portion of the deck 5.25 N/mm (30 lb/in.) were applied to the steel beam (representative formwork) attached to the horizontal legs of the brackets. The load from the finishing screed plays a very important role and acts as a concentrated load for any cross section of the bridge. In this bridge model, the screed machine load was divided equally and applied as a point load at the location of the screed rails. A simply-supported continuous bridge was assumed in simulating the boundary conditions. For any particular section, the considered screed load is 3266 kg (7200 lb) which was divided into two parts applied as a point load on both overhang brackets.

5.2. Transverse rotational comparison between field data and FE result

At section S1 (shown in Fig. 23), a comparative study between field data and FE results is shown for three locations including (i) the bottom flange of the exterior girder, (ii) the web of the exterior girder, and (iii) the bottom flange of the first interior girder. A comparison of the maximum rotations in bottom flange observed in the field and calculated where the finite element model at the west end are very close with values of 0.19° and 0.189°, respectively. The stable rotations were not as close with the finite element model results approximately half of the field monitored data. Since there was no field rotation data for the

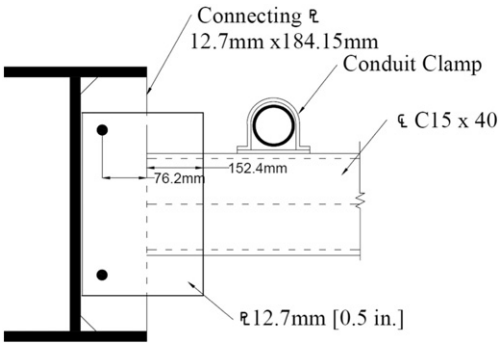

Fig. 10. Detailing of diaphragm.

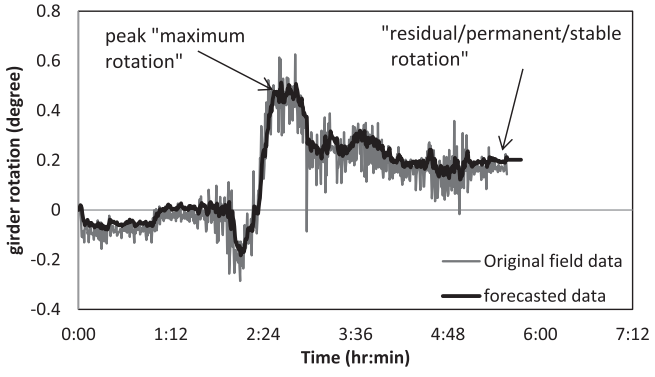

Fig. 11. Finding maximum and stable rotation by simple exponential smoothing.

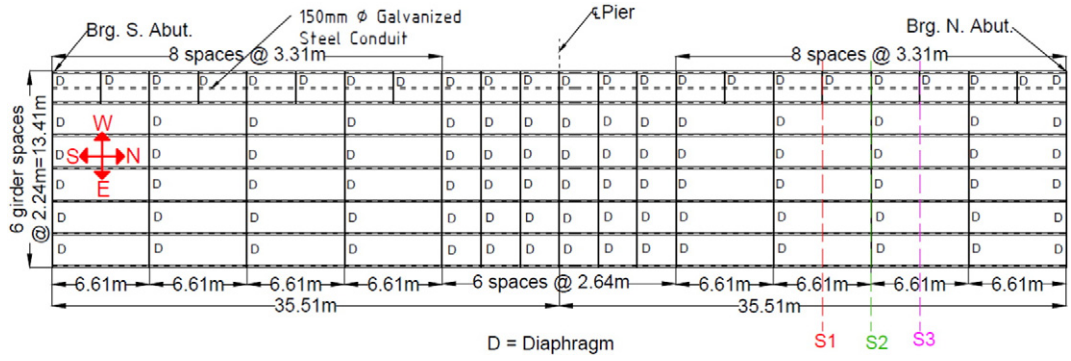

Fig. 12. Predefined sections for instrumentation.

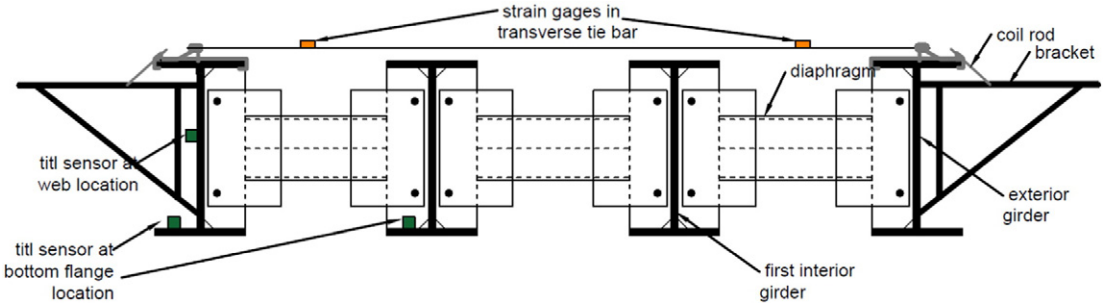

Fig. 13. Location of tilt sensors and strain gages for a bridge with transverse tie arrangement.

east end, girder rotation was calculated from the finite element model. Maximum and stable rotations at the bottom flange were calculated to be 0.23° and 0.13°, respectively. A small difference was observed between the field data and the finite element result for the west side of the exterior girder web for both the maximum (0.22° and 0.223°, respectively) and stable rotation (0.14° and 0.11°, respectively). The calculated maximum and stable rotations in the east end of the deck without intermediate diaphragms were 0.47° and 0.23°, respectively. These rotations are considerably higher than the rotations determined in the west end due to the absence of the intermediate diaphragms. The first interior girder experienced comparatively less rotations than the exterior girders. At the west end, the maximum rotations obtained from the field and the finite element are similar, but the stable rotations predicted by the finite element analysis is approximately 40% less than the field rotation. Since there was no tilt sensors installed on the east end of the girder, the girder maximum and stable rotation was extrapolated from the finite element analysis, and found to be 0.16° and 0.03°, respectively.

A comparison between rotations collected in the field and from the finite element model is shown in Fig. 24 for the bottom flange and web of the girder at section S2. Both east and west ends of the bridge were instrumented with tilt sensors at two different locations on the exterior girders including (i) the bottom flange of the exterior girder, and (ii) the web of the exterior girder. The bottom flange maximum rotations calculated from the finite element analysis for both east and west ends are similar (0.18° and 0.22°, respectively) and reasonably close to the field data. The stable rotations of the exterior bottom flange at the west and east ends measured from the field, are higher than the rotations from the finite element result by 64% and 26.31%, respectively. Rotations from the finite element model at the web are nearly the same as the rotations at the bottom flange for both east and west sides of the bridge. But in the case of stable rotations, when compared with the field

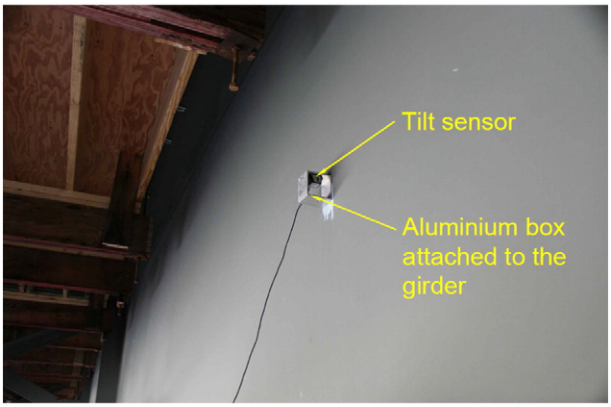

Fig. 14. Installed tilt sensor to the web of the girder.

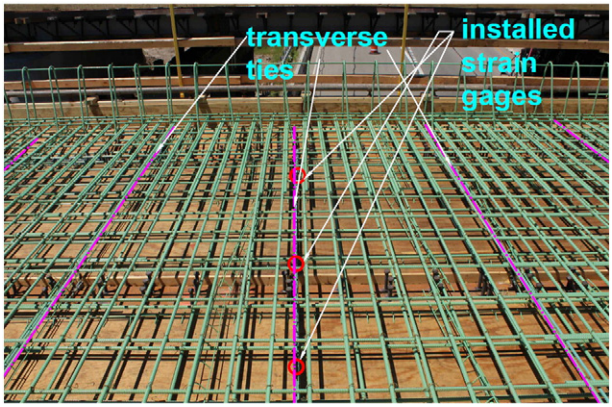

Fig. 15. Installed strain gage to the transverse tie bar.

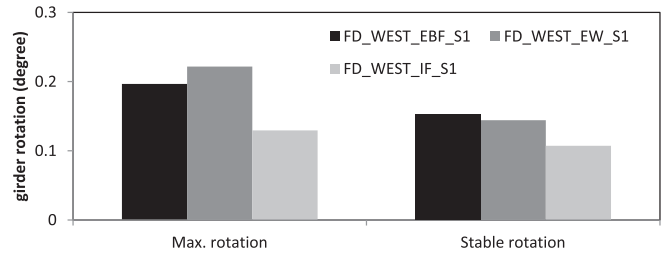

* ***FD:*** *Field data,* ***EBF:*** *Exterior girder bottom flange,*
EW: *Exterior girder web,* ***IF:*** *Interior girder bottom flange*

Fig. 16. Field monitored transverse rotations at section: S1.

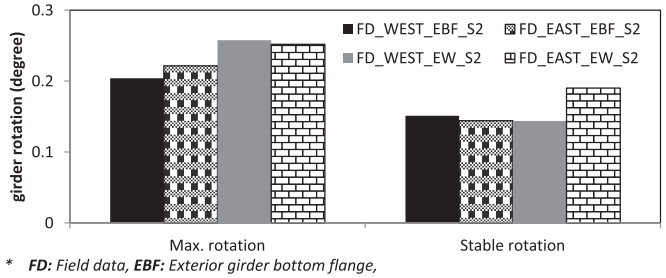

* ***FD:*** *Field data,* ***EBF:*** *Exterior girder bottom flange,*
EW: *Exterior girder web*

Fig. 17. Field monitored transverse rotations at section: S2.

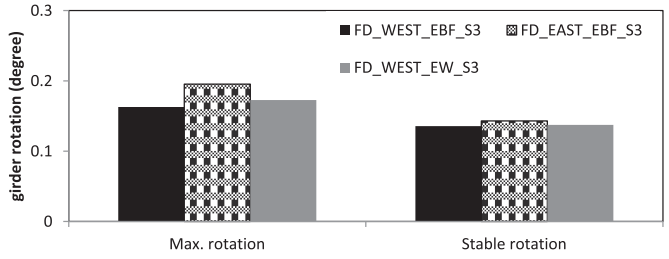

* ***FD:*** *Field data,* ***EBF:*** *Exterior girder bottom flange,*
EW: *Exterior girder web*

Fig. 18. Field monitored transverse rotations at section: S3.

data, rotations are 47.42% (west end) and 35.71% (east end) greater than the rotations from the finite element analysis.

A comparison between field data and FE results for transverse rotations at section S3 for two different locations on the exterior girder is shown in Fig. 25 including (i) bottom flange: the maximum rotations from field data and finite element results are very close at both east and west ends where in west end. On the other hand, in the case of

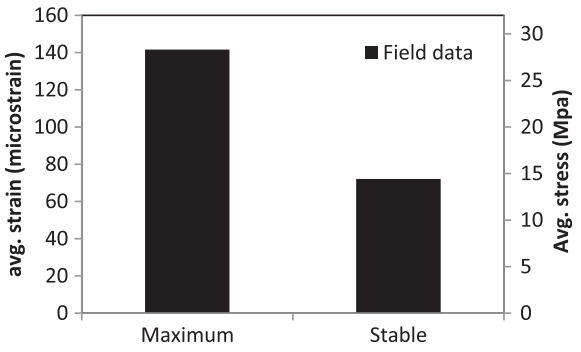

Fig. 20. Field monitored average stress/strain data in transverse tie bars.

stable rotation, FE rotations are 9.25% and 12.82% greater than the field rotations in west and east exterior girders of the bridge, respectively. (ii) Web of the girder: it can be seen from both field data and finite element result that there is no big difference in maximum rotations at the west end, but in the case of stable rotations, the FE rotation is 57% smaller than the field value. In the east end of the bridge, there was no tilt sensor installed at the web location but the FE maximum and stable rotations are 0.42° and 0.22°, respectively. Rotations are even much bigger than the field rotations at the bottom flange.

It was observed in Figs. 23 and 25, the maximum rotations at web location of east exterior girder exceeded the "limit rotation". The calculated maximum rotations (at the web location of the east exterior girder) at section S1 and S3 are respectively 56.67% and 40% larger than the "limit rotation". It means that the applied rotation prevention systems (tie bars and timber blocks) for this bridge were not effective and appropriate. On the other hand, extra intermediate diaphragms played significant job in preventing exterior girder rotation in the west end because all the field and FE rotation were below the allowable rotation.

5.3. Stress/strain value comparison between field data and FE result

Comparison between field data and FE results for stress/strain in transverse tie bars is shown in Fig. 26. The monitored average maximum strain/stress in the field is approximately 25% larger than the finite element value but the average field stable rotation is considerably bigger than the FE result.

5.4. Parametric studies

Two important parameters were studied and conducted basically to check the following two points: (i) the maximum rotations in exterior girders when there is no rotation prevention system (tie bars and timber blocks); (ii) the effect of fully engaged (no sagging in the tie bars and timber blocks are considered as perfectly shimmed) rotation prevention systems to the exterior girders; (iii) efficiency of intermediate diaphragms as a replacement of applied rotation prevention system (tie bars and timber blocks).

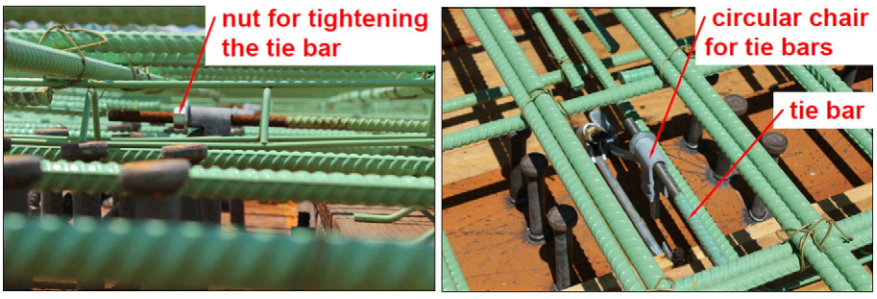

Fig. 19. Dayton's steel hangers used to attach the transverse tie bars with the exterior girders.

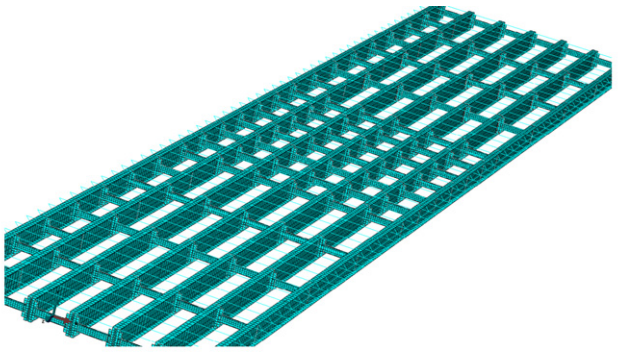

(a) Full scale finite element model for the bridge

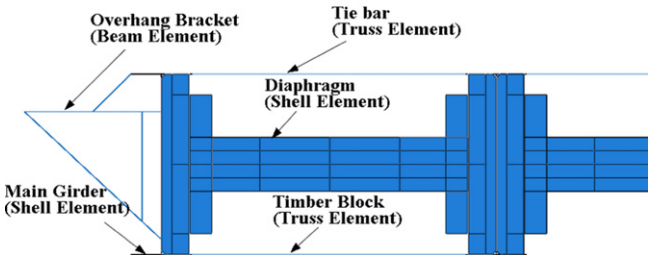

(b) Cross sectional view of exterior girder with first interior girder

Fig. 21. Full scale finite element model for the bridge.

In Fig. 27, when all the rotation prevention systems/elements (tie bars and timber blocks) were assumed in the finite element model to be fully engaged, the calculated maximum rotations at section S1 (mid-span) were much smaller than the monitored field data in the west and east exterior girders, respectively. Again the maximum rotations in west exterior girder are comparatively smaller than the rotation in east exterior girder. Especially, in the case of east exterior girder at web location, the maximum rotation exceeded the "limit rotation". That was happened in west exterior girder due to the effect of combined action of the intermediate diaphragm and the fully engaged rotation prevention systems/elements assumed in the FE model. In this case, tie bars and timber blocks worked as a perfectly tension and compression carrying members respectively. On the other hand, there is no intermediate diaphragm in the east exterior panel and the maximum rotations at the bottom flange and web location in east exterior girder are almost two times larger than the west exterior girder. This indicated effect and importance of intermediate diaphragm in the exterior panels as a rotation preventer.

Fig. 28 illustrates the maximum rotations in exterior girders at the section S1 without considering any rotation prevention systems/elements (tie bars and timber blocks) in the bridge. In this case, diaphragms were effective as major rotation prevention elements. Therefore, it is important to analyze Fig. 28 to understand the insight role of the intermediate diaphragms as a rotation preventer. In the case of west exterior girder, the FE maximum rotations at both bottom flange and web location of the girder showed smaller rotation but slightly (20% for the bottom flange and 45% for web location) higher than the monitored field rotation. Looking at the maximum rotation in west exterior girder at web location, the rotation is slightly above the

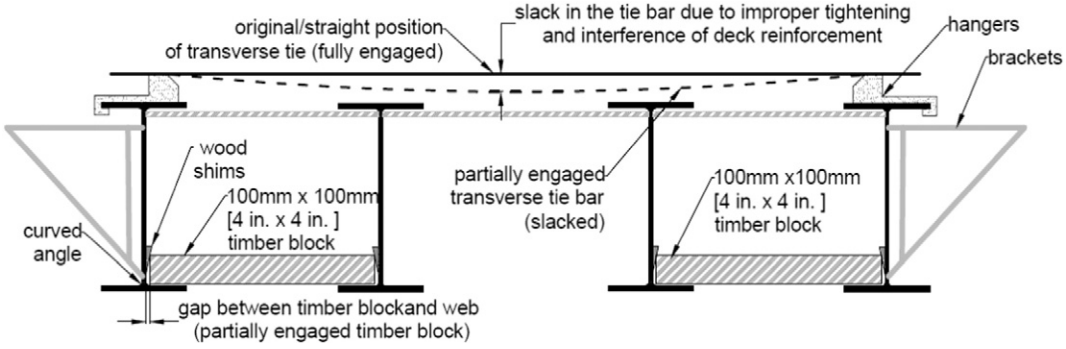

Fig. 22. Gap in between girder and timber blocks due to curved corner.

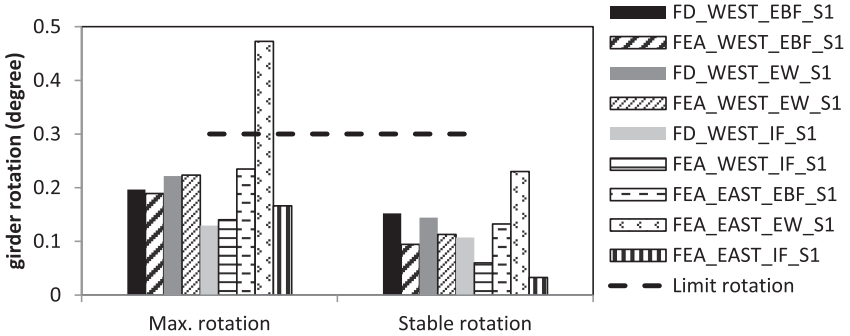

* ***FD:*** *Field data,* ***FEA:*** *Finite element analysis,* ***EBF:*** *Exterior girder bottom flange,* ***EW:*** *Exterior girder web,* ***IF:*** *Interior girder bottom flange*

Fig. 23. Comparison between field data and FE results for transverse rotations at section: S1.

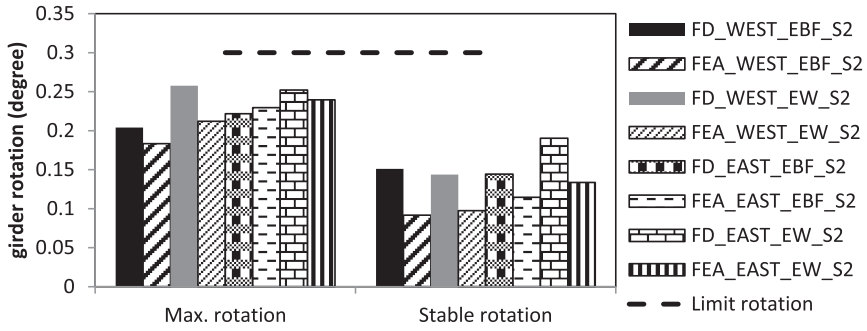

* ***FD:*** *Field data,* ***FEA:*** *Finite element analysis,* ***EBF:*** *Exterior girder bottom flange,* ***EW:*** *Exterior girder web,*

Fig. 24. Comparison between field data and FE results for transverse rotations at section: S2.

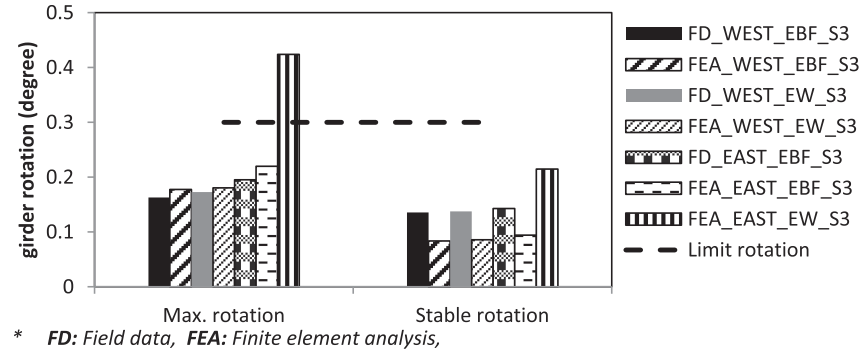

* ***FD:*** *Field data,* ***FEA:*** *Finite element analysis,*
EBF: *Exterior girder bottom flange,* ***EW:*** *Exterior girder web,*

Fig. 25. Comparison between field data and FE results for transverse rotations at section: S3.

"limit rotation". It means that there is no significant effect from tie bar or timber blocks once the intermediate diaphragms are used. On the other hand, the FE maximum rotation in the east exterior girder showed large rotation which is around 1.5 times greater than extrapolated field data (shown in Fig. 23). And both maximum rotations at the bottom flange and web location showed much higher rotation than "limit rotation". This is attributed to the absence of additional intermediate diaphragm between the normal continuous diaphragms. It means that diaphragm spacing in the exterior panels are really important to prevent exterior girder rotation. However the connection or engagement of tie bars has to ensure during construction. Otherwise, tie bars cannot show the effective performance. In contrast, it is really practically difficult to tighten the nuts equally during installation of the tie bars and also a complex task to nullify the sagging in the tie bars.

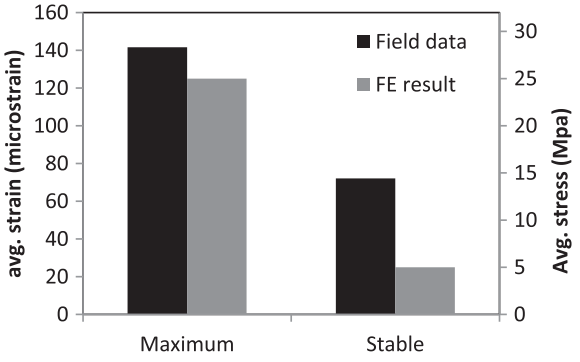

Fig. 26. Comparison between field data and FE results for stress/strain in transverse tie bars.

6. Conclusions

This research focuses on exterior girder rotations in a medium size plate girder bridge with asymmetric end diaphragms due to overhang construction loadings. The following conclusions can be drawn based on the monitored field data and finite element analysis results: Exterior girders at the west end experienced almost a rigid body rotation due to the closely spaced diaphragms but on the other hand the exterior girder at the east end (where fewer diaphragms exist) experienced differential rotation between the web and the bottom flange. Therefore it can be deduced that diaphragm spacing has a significant impact on the behavior of exterior girder rotations during bridge deck construction.

i. At sections where continuous diaphragms exist, girder rotations were comparatively smaller with a rigid body rotation (difference in rotation between the flange and the web is not significant).
ii. Although, there is no tilt sensor installed at section S1, the predicted maximum rotation from the finite element analysis was 0.47° which occurred at the mid span of the bridge at the east end.
iii. Comparing east and west exterior girders, it was found that the presence of continuous intermediate diaphragms can make a significant change in rotational stiffness and behavior.
iv. The maximum measured exterior girder rotation from the finite element analysis is 0.47° which occurred at the web location at

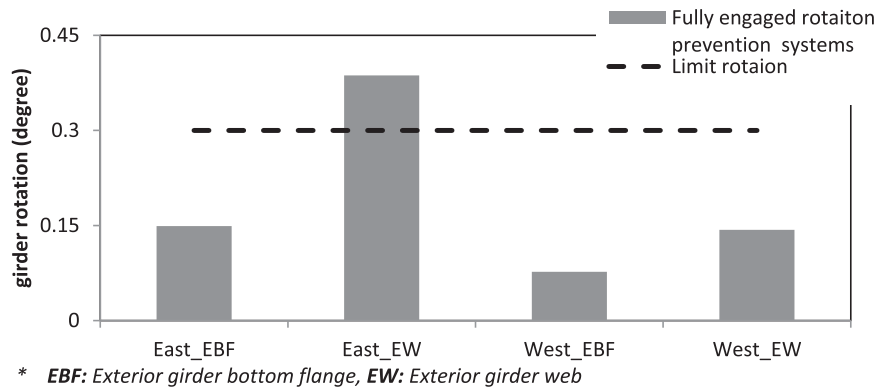

Fig. 27. Rotations in exterior girders considering rotation prevention systems are fully engaged.

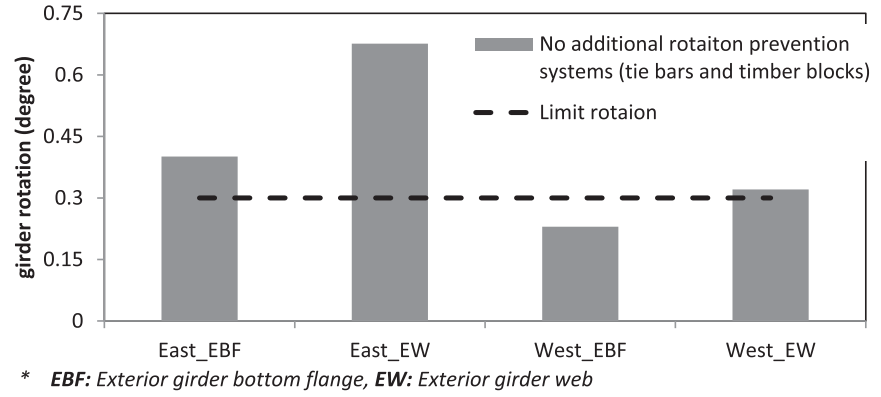

Fig. 28. Rotations in exterior girders considering no rotation prevention systems.

mid span of the bridge at the east end without a diaphragm and the calculated rotation exceeds the assigned limit rotation (θ).

v. Field stable rotations are higher (approximate 50% on average) than rotation determined from the finite element study. These larger stable rotations were seen in the exterior girders as a result of permanent deformation occurring when the finishing screed passed by the section under consideration.
vi. Based upon field and finite element analysis, it was found that the additional intermediate diaphragms (at west end) have tremendous ability to prevent exterior girder rotation during overhang deck construction.
vii. It was observed in the field that proper tightening of the long and continuous tie bars is difficult because of their interference with other deck reinforcement, and the timber blocking was also frequently improperly shimmed. Improper installation of these elements greatly reduces or eliminates their effectiveness.
viii. It was found from the FE parametric studies that fully engaged tie bars and timber blocks work effectively to prevent/decrease exterior girder rotation. In order to consider the feasibility issue for tie bars and timber blocks, further study is needed.

References

[1] Fasl J. The influence of overhang construction on girder design. [Ph.D. Thesis] Texas, U.S.A.: University of Texas at Austin; 2008
[2] Maiorana E, Pellegrino C, Modena C. Elastic stability of plates with circular and rectangular holes subjected to axial compression and bending moment. Thin-Walled Struct 2009;47(3):241–55.
[3] Xie M, Chapman JC. Design of web stiffeners: local panel bending effects. J Constr Steel Res 2004;60(10):1425–52.
[4] Shokouhian M, Shi Y. Flexural strength of hybrid steel I-beams based on slenderness. Eng Struct 2015;93:114–28.
[5] Gupta VK, Okui Y, NAGAI M. Development of web slenderness limits for composite I-girders accounting for initial bending moment. Struct Eng/Earthq Eng 2006;23(2):229S–39S.
[6] Sayed-Ahmed EY. Lateral torsion-flexure buckling of corrugated web steel girders. Proc ICE-Struct Build 2005;158(1):53–69.
[7] Kala Z, Kala J, Melcher J, Skaloud M, Omishore A. Imperfections in steel plated structures–should we straighten their plate elements? Nordic steel construction conference 2009; 2009.
[8] Yang S, Helwig T, Klingner R, Engelhardt M, Fasl J. Impact of overhang construction of girder design. Technical report no. FHWA/TX-10/0-5706-1. Texas, U.S.A.: Texas Department of Transportation; 2010
[9] Haskett M, Oehlers DJ, Ali MM, Wu C. Rigid body moment–rotation mechanism for reinforced concrete beam hinges. Eng Struct 2009;31(5):1032–41.
[10] Ariyasajjakorn D. Full scale testing of overhang falsework hangers on NCDOT modified bulb tee (MBT) girders. [Master's Thesis] North Carolina, U.S.A.: North Carolina State University; 2006
[11] Clifton SP, Bayrak O. Bridge deck overhang construction. Technical report no. IAC 88-5DD1A003-2. Texas, U.S.A.: Texas Department of Transportation; 2008
[12] Grubb M. Design for concrete deck overhang loads. Final report. AISC Marketing Inc.; 1990
[13] Schilling CG. Moment-rotation tests of steel bridge girders. J Struct Eng 1988 1988;114(1):134–49.
[14] Ito M, Nozaka K, Shirosaki T, Yamasaki K. Experimental study on moment–plastic rotation capacity of hybrid beams. J Bridg Eng 2005;10(4):490–6.
[15] Ito M, Karatani E, Komuro Y. Moment-inelastic rotation behavior of longitudinally stiffened beams. J Bridg Eng 2002;7(4):223–8.
[16] Helwig T, Yura J. Steel bridge design handbook: bracing system design. Report no. FHWA-IF-12-052-Vol. 13. Washington, DC, U.S.A.: Federal Highway Administration; 2012
[17] Roddis WK, Baghernejad S, Winters EL. Cross-frame diaphragm bracing of steel bridge girders. Technical report no. K-TRAN: KU-01-2. Kansas, U.S.A.: Kansas Department of Transportation; 2008
[18] Suprenant B. Setting screed rails for bridge deck paving, concrete construction. Concrete construction. The Aberdeen Group; 1994.
[19] Green T, Yazdani N, Spainhour L. Contribution of intermediate diaphragms in enhancing precast bridge girder performance. J Perform Constr Facil 2004;18(3):142–6.
[20] Brown RG, Meyer RF. The fundamental theorem of exponential smoothing. Oper Res 1961 1961;9(5):673–85.
[21] Dayton Superior Corporation. Bridge deck handbook; 2015.